Available online at www.sciencedirect.com
ScienceDirect
Ceramics International 37 (2011) 3687–3690
CERAMICS INTERNATIONAL
www.elsevier.com/locate/ceramint

Multiferroic properties of single-crystalline $Bi_{0.8}La_{0.2}FeO_3$ microsized particles synthesized by molten salt method

L. Zhai [a], Y.G. Shi [b], J.L. Gao [a], S.L. Tang [a,*], Y.W. Du [a]

[a] National Laboratory of Solid State Microstructures, Nanjing University, Nanjing 210093, China
[b] Department of Applied Physics, Nanjing University of Aeronautics and Astronautics, Nanjing 210016, China

Received 29 March 2011; received in revised form 6 June 2011; accepted 16 June 2011
Available online 23 June 2011

Abstract

Single-crystalline $Bi_{0.8}La_{0.2}FeO_3$ particles were successfully synthesized by a large scale, facile and environmentally friendly molten salt method. The structure, morphology, magnetic and ferroelectric properties were investigated. The X-ray diffraction results demonstrate that the sample was almost single phase with a rhombohedral structure. The morphology studies show that $Bi_{0.8}La_{0.2}FeO_3$ particles are mainly cubic with an average size of 2 μm. The room-temperature field dependence of magnetization for the $Bi_{0.8}La_{0.2}FeO_3$ exhibits a hysteresis behavior. The temperature dependence of magnetization indicates the magnetic ordering temperature is 660 K. The ferroelectric properties of $Bi_{0.8}La_{0.2}FeO_3$ particles were investigated by piezoreponse force microscopy.

PACS : 75.85.+t; 77.80.−e; 75.50.Ee

Keywords: Multiferroic; $BiFeO_3$; Magnetization; Ferroelectricity

1. Introduction

Multiferroic materials, combining more than one ferroic order simultaneously, have attracted an ever-increasing attention in recent years due to the potential applications in sensors, data storage devices, transducers, etc. [1–4]. Among these multiferroic materials, $BiFeO_3$, crystallized in ABO_3-typed perovskite structure with *R*3*c* space group at room temperature, shows both high ferroelectric Curie temperature $T_c \sim 1103$ K and antiferromagnetic Néel temperature $T_N \sim 657$ K [5,6]. These specific features for $BiFeO_3$ are advantageous for basic research and various applications. However, $BiFeO_3$ is metastable in air. The kinetics of phase formation in the Bi_2O_3–Fe_2O_3 system can easily lead to the appearance of unwanted phases, such as $Bi_2Fe_4O_9$ and $Bi_{25}FeO_{40}$ [7,8], which causes the reduced resistivity and inferior ferroelectric properties in $BiFeO_3$. On the other hand, the magnetic structure of $BiFeO_3$ is antiferromagnetic with G-type ordering. This G-type antiferromagnetic is slightly modulated to a cycloidal spiral structure with a period of 62 nm length with [1 1 0] as the spiral propagation direction and spin rotation within (1 1 0), thereby producing a helimagnetic order and a vanishing magnetization in the bulk [9]. Therefore, much attention has been paid to stabilize the phase and improve the multiferroic properties of $BiFeO_3$ [10–17]. Previous studies indicated that the doping of lanthanide ions La^{3+} was an effective way to enhance the insulating and ferroelectric properties by the reduced oxygen vacancy. In addition, the space-modulated spin structure of $BiFeO_3$ can be effectively suppressed by the substitution of La^{3+}. Sosnowska et al. investigated the influence of La^{3+} on magnetic properties of $BiFeO_3$ by means of Neutron diffraction studies [12]. They found that the span of magnetic satellites becomes narrower and the magnetic cycloid becomes longer in La-doped $BiFeO_3$ alloys. Thus, partial substitution of Bi^{3+} by La^{3+} could improve ferroelectric and magnetic properties of $BiFeO_3$ simultaneously. In the present work, single-crystalline $Bi_{0.8}La_{0.2}FeO_3$ microsized particles were successfully synthesized by a large scale, facile and environmentally friendly molten-salt synthesis (MSS) method. The structure, morphology, mechanism of crystal growth, magnetic and ferroelectric properties are reported.

* Corresponding author. Tel.: +86 25 83593817; fax: +86 25 83595535.
E-mail address: tangsl@nju.edu.cn (S.L. Tang).

0272-8842/$36.00
doi:10.1016/j.ceramint.2011.06.030

2. Experiment

The starting materials Bi_2O_3, La_2O_3, Fe_2O_3, NaCl, all with a purity of 99.99%, were used to synthesize $Bi_{0.8}La_{0.2}FeO_3$ particles. Bi_2O_3, La_2O_3, Fe_2O_3 were weighted by stoichimetric ratio of $Bi_{0.8}La_{0.2}FeO_3$ as raw materials and the NaCl was weighted as the solvent. The mole ratio of $Bi_{0.8}La_{0.2}FeO_3$ to the flux was 1:20. Then the raw materials and solvent were grounded for 20 min. The reactant mixtures were placed inside an alumina crucible and heated at 800 °C for 30 min before quenching to the room temperature. The desired $Bi_{0.8}La_{0.2}FeO_3$ products were obtained after washing the quenched material several times with deionized water to remove NaCl.

Conventional X-ray diffraction (XRD) analysis was carried out using Cu $K\alpha$ radiation with a Rigaku D/Max-gA diffractometer. The morphology of $Bi_{0.8}La_{0.2}FeO_3$ powders was studied by field emission scanning electron microscopy (FE-SEM). Magnetic properties of the sample were investigated with a superconducting quantum interference device (SQUID) magnetometer. The ferroelectric properties of $Bi_{0.8}La_{0.2}FeO_3$ microcrystals were investigated by a piezoresponse force microscopy (PFM, Digital Instruments, Nano-Scope V, Veeco) equipped with a Pt/Ir coated Cr tip. The tip radius was less than 20 nm and a force constant of 4 N/m was use to study the piezoresponse of the regions without top electrodes.

3. Results and discussion

Fig. 1 shows the XRD patterns of $Bi_{0.8}La_{0.2}FeO_3$ synthesized by MSS method. It can be seen that the sample is almost single phase, and the XRD pattern can be indexed based on the rhombohedral structure. This is consistent with the structure of the La^{3+} doped $BiFeO_3$ bulk compound [13,14]. Because $LaFeO_3$ is much easier to be synthesized than $BiFeO_3$, the stabilization of $Bi_{0.8}La_{0.2}FeO_3$ should be ascribed to the partial substitution of La for Bi. The lattice parameters derived from the XRD patterns are $a = b = 5.587$ and $c = 13.847$ Å, respectively. Attention should be paid that the synthesis temperature in the present work is 800 °C, which is lower than the temperature (generally 860–900 °C) in the traditional solid state reaction method [13,14]. This should be ascribed to the enhanced diffusion coefficients in molten chloride liquid phase compared with that in the solid state [18]. Therefore, MSS method is an effective way to obtain $BiFeO_3$-based compounds at low temperature.

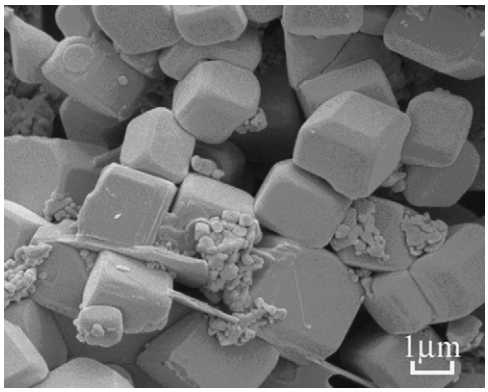

Fig. 2. FE-SEM image of $Bi_{0.8}La_{0.2}FeO_3$ particles.

Fig. 2 presents the FE-SEM images of $Bi_{0.8}La_{0.2}FeO_3$ crystals. It can be seen that $Bi_{0.8}La_{0.2}FeO_3$ mainly consists of cubic crystals with truncated edges and corners. The average size of $Bi_{0.8}La_{0.2}FeO_3$ particles is about 2 μm. The formation of $Bi_{0.8}La_{0.2}FeO_3$ in molten salt can be divided into two processes: nucleation process and growth process. In the first process, the raw materials rearrange and diffuse quickly in a liquid state of the salts when the temperature increases above the melting point of NaCl. Thus, small and aggregated $Bi_{0.8}La_{0.2}FeO_3$ particles are rapidly formed in this period. In the following growth process, the smaller $Bi_{0.8}La_{0.2}FeO_3$ particles gradually dissolve into the NaCl flux and redeposit onto the larger ones in accordance with the Ostwald ripening mechanism [19]. As is shown in Fig. 2, some fine particles (about 50 nm) are found to be adhered to the large ones, which directly confirms the above discussions.

Fig. 3 presents the field dependence of magnetization (M–H) curve for $Bi_{0.8}La_{0.2}FeO_3$ up to a field of 50 kOe at 300 K. In contrast with those of the undoped $BiFeO_3$, which only shows a character of almost standard antiferromagnetic behavior at room temperature without any hysteresis, the M–H curves of the sample has a significant linear contribution but exhibits a

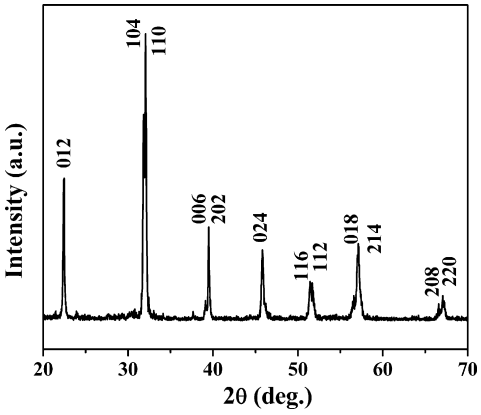

Fig. 1. XRD patterns of $Bi_{0.8}La_{0.2}FeO_3$ particles.

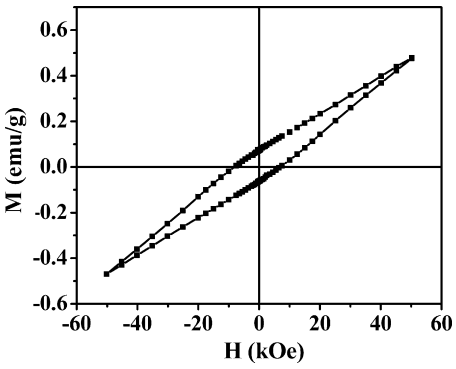

Fig. 3. Magnetic hysteresis loops of $Bi_{0.8}La_{0.2}FeO_3$ particles at 300 K.

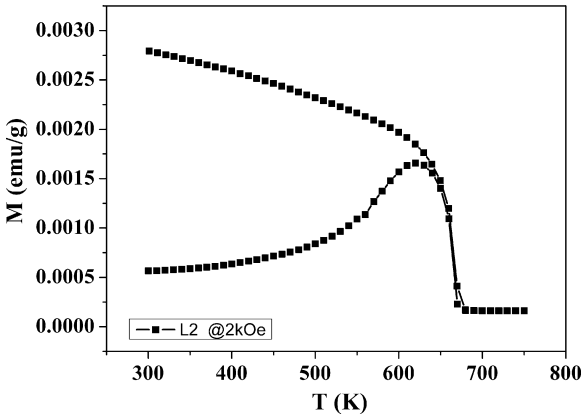

Fig. 4. Temperature dependence of magnetization for $Bi_{0.8}La_{0.2}FeO_3$ particles.

hysteresis behavior. A similar behavior was also observed in $Bi_{0.8}La_{0.2}FeO_3$ bulk materials, which could be associated with the suppressed cycloid spin structure by the introduction of La^{3+} [12,13]. The magnetic remanent magnetization (M_r) and the coercive field (H_c) are 0.07 emu/g and 7.25 kOe, respectively. The M_r is much larger than that of 0.0042 emu/g observed in the corresponding bulk material [14]. As we know, the finite-sized effect at the nanoscale could destroy the spiral spin structure and produce the uncompensated spins at the surface, which increases the net magnetization[20,21]. Therefore, the observed improvement of the magnetic properties in the present sample could be ascribed to the coexistence of the fine particles with a size below 62 nm.

Fig. 4 shows the temperature dependence of magnetization (M–T) of $Bi_{0.8}La_{0.2}FeO_3$ measured at the magnetic field of 2 kOe. The magnetization increases first with the temperature increasing from 300 K to 660 K, which indicates that the ordered spin structure is gradually destroyed with the increasing temperature. The magnetic moments of the sample change sharply near 660 K, at which is the Néel temperature of $Bi_{0.8}La_{0.2}FeO_3$. The divergence between FC and ZFC magnetization curves is due to the large coercivity of $Bi_{0.8}La_{0.2}FeO_3$ [22]. Above the Néel temperature, the magnetization approaches to almost zero, which implies that no other impurity magnetic phase exists. Therefore, the magnetic behavior for the sample at room temperature should come from the $Bi_{0.8}La_{0.2}FeO_3$ phase itself but not the other magnetic impurities.

The ferroelectric properties of $Bi_{0.8}La_{0.2}FeO_3$ microcrystals were investigated at local scale using piezoresponse force microscopy (PFM). A small amount of $Bi_{0.8}La_{0.2}FeO_3$ powders were dispersed in acetone by ultrasonication. Then a few droplets of the resulting suspension were deposited on Pt/Ti/SiO_2/Si substrate and dried. To avoid the uncontrolled displacement of the $Bi_{0.8}La_{0.2}FeO_3$ particles during the measurement, the substrate was thermally treated for 2 h at 500 °C to induce adhesion of the $Bi_{0.8}La_{0.2}FeO_3$ particles. During the measurement, we chose some smooth and clean spots to perform the measurements. Fig. 5(a) and (b) gives the typical topographic and vertical piezoresponse images of $Bi_{0.8}La_{0.2}FeO_3$ particles which was detected by AFM and PFM,

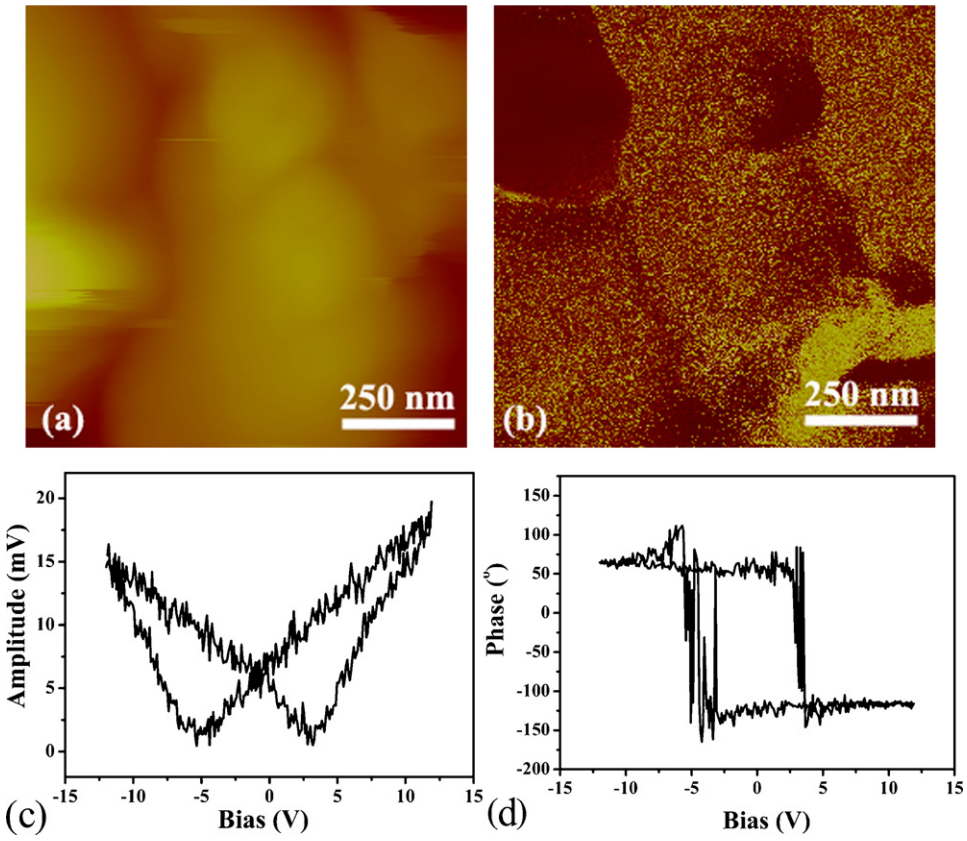

Fig. 5. (a) The topography and (b) the corresponding vertical piezoresponse images of $Bi_{0.8}La_{0.2}FeO_3$ crystals; (c) PFM amplitude–voltage hysteresis loop and (d) PFM phase-voltage hysteresis loop for an individual $Bi_{0.8}La_{0.2}FeO_3$ particle.

respectively. The random distributed particles can be seen in Fig. 5(a). On the corresponding piezoresponse images Fig. 5(b), areas with opposite piezoelectric constants and polarities appear as bright and dark regions. Due to the random crystal orientations of the particles, the piezoresponse of the adjacent parts of neighbouring grains with different polarizations direction are clearly observed.

In order to study the ferroelectric properties of an individual $Bi_{0.8}La_{0.2}FeO_3$ particle, the local hysteretic loops were measured through the local piezoelectric response versus applied voltage. Fig. 5(c) and (d) illustrate the typical piezoresponse results for an individual particle. A classic ''butterfly shape'' amplitude–voltage loop (Fig. 5(c)) and a square phase-voltage loop (Fig. 5(c)) were observed, which confirms the ferroelectric nature of the $Bi_{0.8}La_{0.2}FeO_3$ crystals. By sweeping the amplitude of the AC testing signal from 0 to 10 V, the effective piezoelectric coefficient d_{33} can be obtained from the slope of the acquired piezoresponse amplitude versus AC amplitude curve. Here, the effective piezoelectric coefficient d_{33} of $Bi_{0.8}La_{0.2}FeO_3$ crystal is estimated to be around 11 pm/V.

4. Conclusion

A large scale, facile and environmentally friendly molten salt method were employed to synthesize the single-crystalline $Bi_{0.8}La_{0.2}FeO_3$ microsized particles. The FE-SEM image shows the average size of the sample is about 2 μm with some small particles adhering to large ones, which reveals that the crystal growth follows the Ostwald mechanism. The temperature dependence of magnetization indicates the Néel temperature of the sample is 660 K. The PFM measurements confirm the nature of ferroelectric of our sample. The effective piezoelectric coefficient d_{33} is estimated to be around 11 pm/V.

Acknowledgements

This work is supported by National Key Project of Fundamental Research of China (Nos 2005CB623605 and 2010CB923404).

References

[1] J. Wang, J.B. Neaton, H. Zheng, V. Nagarajan, S.B. Ogale, B. Liu, D. Viehland, V. Vaithyanathan, D.G. Schlom, U.V. Waghmare, N.A. Spaldin, K.M. Rade, M. Wutting, R. Ramesh, Epitaxial $BiFeO_3$ multiferroic thin film heterostructures, Science 299 (2003) 1719–1722.

[2] T. Zhao, A. Scholl, F. Zavaliche, K. Lee, M. Barry, A. Doran, M.P. Cruz, Y.H. Chu, C. Ederer, N.A. Spaldin, R.R. Das, D.M. Kim, S.H. Baek, C.B. Eom, R. Ramesh, Electrical control of antiferromagnetic domains in multiferroic $BiFeO_3$ films at room temperature, Nat. Mater. 5 (2006) 823–829.

[3] Y.H. Chu, L.W. Martin, M.B. Holcomb, M. Gajek, S.J. Han, Q. He, N. Balke, C.H. Yang, D. Lee, W. Hu, Q. Zhan, P.L. Yang, A. Fraile-Rodriguez, A. Scholl, S.X. Wang, R. Ramesh, Electric-field control of local ferromagnetism using a magnetoelectric multiferroic, Nat. Mater. 7 (2008) 478–482.

[4] S. Lee, W. Ratcliff, S.W. Cheong, V. Kiryukhin, Electric field control of the magnetic state in $BiFeO_3$ single crystals, Appl. Phys. Lett. 92 (2008) 192906.

[5] C. Michel, J.M. Moreau, G. Achenbach, R. Gerson, W. James, The atomic structure of $BiFeO_3$, Solid State Commun. 7 (1969) 701–704.

[6] F. Kubel, H. Schmid, Structure of a ferroelectric and ferroelastic monodomain crystal of the perovskite $BiFeO_3$, Acta Crystallogr. Sect. B 46 (1990) 698–702.

[7] M. Kumar, V. Palkar, K. Srinivas, S. Suryanarayana, Ferroelectricity in a pure $BiFeO_3$ ceramic, Appl. Phys. Lett. 76 (2000) 2764–2766.

[8] G. Achenbach, W. James, R. Gerson, Preparation of single-phase polycrystalline $BiFeO_3$, J. Am. Cerm. Soc. 50 (1967) 437.

[9] I. Sosnowska, T. Neumaier, E. Steichele, Spiral magnetic ordering in bismuth ferrite, J. Phys. C: Solid State Phys. 15 (1982) 4835–4846.

[10] I. Sosnowska, W. Schäfer, W. Kockelmann, K.H. Andersen, I.O. Troyanchuk, Crystal structure and spiral magnetic ordering of $BiFeO_3$ doped with manganese, Appl. Phys. A: Mater. Sci. Process. 74 (2002) S1040–S1042.

[11] W.A. Murashov, D.N. Rakov, I.S. Dubienko, A.K. Zvezdin, W.M. Ionov, Segnietietomagnetism in crystals of alloys (Bi,La)FeO_3, Sov. Krystalografia 35 (1990) 912–917.

[12] I. Sosnowska, M. Loewenhaupt, W.I.F. David, R.M. Ibberson, Searching for the magnetic spiral arrangement in $Bi_{1-x}La_xFeO_3$, Mater. Sci. Forum 133–136 (1993) 683–685.

[13] Y.H. Lin, Q.H. Jiang, Y. Wang, C.W. Nan, L. Chen, J. Yu, Enhancement of ferromagnetic properties in $BiFeO_3$ polycrystalline ceramic by La doping, Appl. Phys. Lett. 90 (2007) 172507.

[14] S.T. Zhang, Y. Zhang, M.H. Lu, C.L. Du, Y.F. Chen, Z.G. Liu, Y.Y. Zhu, N.B. Ming, X.Q. Pan, Substitution-induced phase transition and enhanced multiferroic properties of $Bi_{1-x}La_xFeO_3$ ceramics, Appl. Phys. Lett. 88 (2006) 162901.

[15] L. Zhai, Y.G. Shi, S.L. Tang, L.Y. Lv, Y.W. Du, Large magnetic coercive field in $Bi_{0.9}La_{0.1}Fe_{0.98}Nb_{0.02}O_3$ polycrystalline compound, J. Phys. D: Appl. Phys. 42 (2009) 165004.

[16] D. Lee, M.G. Kim, S. Ryu, H.M. Jang, S.G. Lee, Epitaxially grown La-modified $BiFeO_3$ magnetoferroelectric thin films, Appl. Phys. Lett. 86 (2005) 222903.

[17] S. Kazhugasalamoorthy, P. Jegatheesan, R. Mohandoss, N.V. Giridharan, B. Karthikeyan, R. Justin Joseyphus, S. Dhanuskodi, Investigations on the properties of pure and rare earth modified bismuth ferrite ceramics, J. Alloys. Compd. 493 (2010) 569–572.

[18] C. Mao, G. Wang, X. Dong, Z. Zhou, Y. Zhang, Low temperature synthesis of $Ba_{0.70}Sr_{0.30}TiO_3$ powders by the molten-salt method, Mater. Chem. Phys. 106 (2007) 164–167.

[19] P. Voorhees, Ostwald ripening of two-phase mixtures, Annu. Rev. Mater. Sci. 22 (1992) 197–215.

[20] T.J. Park, G.C. Papaefthymiou, A.J. Viescas, A.R. Moodenbaugh, S.S. Wong, Size-dependent magnetic properties of single-crystalline multiferroic $BiFeO_3$ nanoparticles, Nano Lett. 7 (2007) 766–772.

[21] R. Mazumder, P.S. Devi, D. Bhattacharya, P. Choudhury, A. Sen, M. Raja, Ferromagnetism in nanoscale $BiFeO_3$, Appl. Phys. Lett. 91 (2007) 062510.

[22] P.A. Joy, S.K. Date, Effect of sample shape on the zero-field-cooled magnetization behavior: comparative studies on $NiFe_2O_4$, $CoFe_2O_4$ and $SrFe_{12}O_{19}$, J. Magn. Magn. Mater. 222 (2000) 33–38.